Broadband Time-domain Terahertz Radar: cross section measurement and imaging

Dachuan Liang[1], Minggui Wei [1], Jianqiang Gu[1], Zhen Tian[1], Chunmei Ouyang[1], Jiaguang Han[1], and Weili Zhang[1,2]

[1]Center for Terahertz Waves and College of Precision Instrument and Optoelectronics Engineering, Tianjin University, and the Key Laboratory of Optoelectronics Information and Technology, Ministry of Education, Tianjin 300072, China

[2]School of Electrical and Computer Engineering, Oklahoma State University, Stillwater, Oklahoma 74078, USA

***Abstract*—Based on a broadband time-domain terahertz radar system, we performed far-field radar cross section measurements of two metal scaled models at terahertz frequencies. The novel broadband radar can provide not only frequency-averaged RCS but also RCS distributions at arbitrary frequency. The measured terahertz RCS of the models can be scaled to that of the full-size real object at conventional radar frequencies. In addition, imaging of the scaled models based on filtered back projection algorithm has been proved to be helpful for finding the main scattering points.**

I. INTRODUCTION

The scattering of terahertz (THz) waves by dielectric and conducting objects has become a booming research topic in THz studies. Recently, terahertz time-domain spectroscopy (THz-TDS) system was introduced to radar cross section (RCS) measurement and radar target imaging [1,2]. Compared with the scaled RCS measurement in microwave frequency domain, THz-TDS radar system operates with shorter wavelengths (30 μm-3mm). On the other hand, both the lateral and axial resolutions of a THz radar are higher than those in a microwave radar, which can be attributed to the smaller wavelength of the THz waves and the broadband feature (0~1.3 THz) of the TDS system.

II. RESULTS

Our THz radar system is based on typical THz-TDS system. Terahertz waves are generated by photoconductive antenna (gallium arsenide). The THz beam is expanded by a pair of off-axis parabolic mirror and spherical mirror with focal lengths of 10.16cm and 60.96cm respectively. This telescope system increases the THz beam size by a factor of 6, which provides an output beam with full width of 120mm [4].

RCS is the measure of a target's ability to reflect radar signals in the direction of the radar receiver, which has units of area (meters squared). Quantitatively, RCS is calculated in three-dimensions as:

$$RCS=\lim_{R\to\infty} 4\pi R^2 \frac{|E_s|^2}{|E_i|^2}, \qquad (1)$$

where E_i and E_s are the incident and scattered electric fields, respectively, and R is the distance between target and radar. The incident wave must be a plane wave in this definition. Our THz radar system can provide collimated THz plane wave and meet the demand.

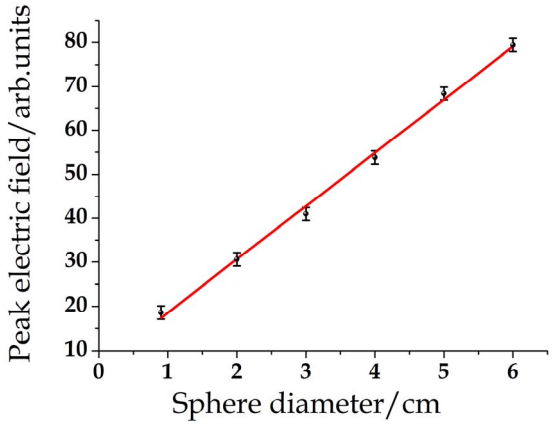

Fig. 1. The peak electric amplitude of THz radiation scattered from six metal spheres with diameter of 0.9 cm, 2 cm, 3 cm, 4 cm, 5 cm, 6 cm, respectively. The red line is the linear fit to the measured data.

Before all the measurement, several perfectly conducting spheres with different radii were used to calibrate the radar system because of its simplest scattering characteristics. Electromagnetic waves scattered by a conducting sphere can be described by Mie theory. For $k \cdot r >> 1$, the *RCS* of a metal sphere is frequency independent and can be expressed as $RCS = \pi \cdot r^2$, where k is the wave number, r is the sphere radius. In our THz radar system, the directly measured signals are time-domain signals so the temporal peak electric amplitude E_p and r holds the relation of E_p~r [2]. The peak scattered electric field of a series of metal spheres of different diameters are measured by our THz radar system. Figure 1 shows this linear relationship of peak scattered electric amplitude and the sphere diameter, which proves the effectiveness of our THz radar system.

In this paper, we adopted a time-domian or say frequency-averaged radar cross section to measure and calculate the *RCS* of the complicated structures [2], it can be defined by:

$$RCS = \pi r_0^{\,2} \cdot \frac{\int_0^T \left|E_{object}(t)\right|^2 dt}{\int_0^T \left|E_{cal}(t)\right|^2 dt - \int_0^T \left|E_{bg}(t)\right|^2 dt}, \qquad (2)$$

where $E_{object}(t)$ is the electric field scattered by object, $E_{cal}(t)$ is the electric field scattered by calibrated spheres, and $E_{bg}(t)$

is background noise. And simply with the Fourier transform, the frequency resolved RCS can also be introduced as:

$$RCS(\omega) = \pi r_0^{\,2} \cdot \frac{\left|\tilde{E}_{object}(\omega)\right|^2}{\left|\tilde{E}_{cal}(\omega)\right|^2 - \left|\tilde{E}_{bg}(\omega)\right|^2}, \quad (3)$$

Where $\tilde{E}_i(\omega)$ is the Fourier transform of $E_i(t)$.

The frequency-averaged RCS for a 1:2000 scaled Liaoning aircraft carrier metal model is shown in Fig. 2a. At 1/2000 scale, the inversely calculated radar frequency is 0.05-0.7 GHz (L-band). From Fig. 2a, we can see that the largest RCS is obtained at the angle that the deck of the airplane is exposed to the THz radiation directly due to its flat shape (0^0- direction). At 90^0-direction, another maximal value can be observed, which largely results from the scattering of the ship island. The RCS distribution is asymmetric due to the asymmetric

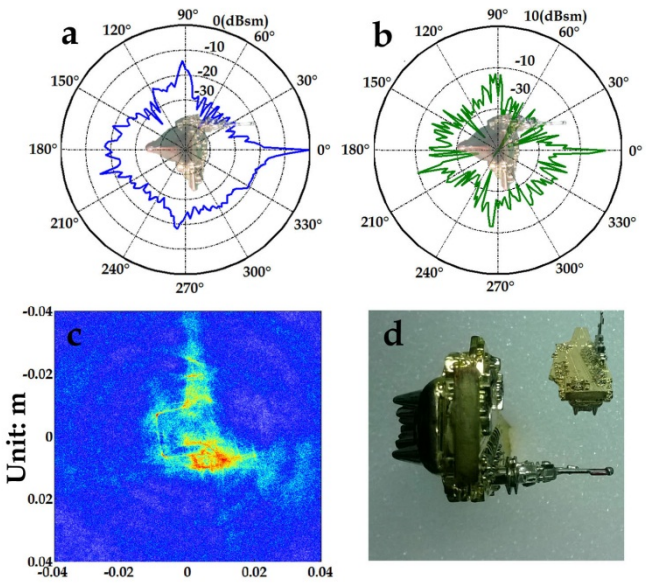

Fig. 2. (a) Frequency-averaged RCS of the model of the aircraft carrier. (b) Frequency-resolved RCS of the scaled model at 0.6 THz. (d) cross section image reconstructed using the filtered back projection algorithm. (d) Metal 1:2000 scaled model of Liaoning aircraft carrier.

configuration of the scale model.

Figure 2b presents the frequency-resolved RCS distribution of the model at 0.6 THz. A sharp RCS peak can be observed at 0^0. Other RCS maximal values occur at directions with large plane surfaces like 90^0 and 270^0. The frequency-resolved RCS fluctuates more intensively than the frequency-averaged one. This is because the summation of RCS at different frequencies smoothens the angle dependence of the distribution.

The imaging result of the Liaoning aircraft carrier scaled model is reconstructed by the filtered back projection algorithm (FBP) method as shown in Fig. 2c [2,3]. The shape and profile of the image is very clear and in good accordance with the actual scaled model as shown in Fig. 2d. More importantly, the intensity of each pixel reveals the scattering point distribution on the model. Some particular scattering points, like the deck and hull bottom can be easily distinguished. The outline of the ship island is much more complicated than the other parts; correspondingly the scattering effect is stronger, which can be easily recognized in Fig. 2d.

Fig. 3a shows the frequency-averaged *RCS* for the 1:200 scale model of aircraft fighter F-22. The frequency-resolved RCS distribution of the F-22 model at 0.6 THz is shown in Fig. 3b. At 1/200 scale, the inversely calculated radar frequency is 0.5-7 GHz (L-C band). From the RCS distribution we can see that the largest RCS is obtained at the angle below and above the aircraft. The frequency-averaged RCS distribution is much smoother than the frequency-resolved one because its summation process.

Figure 3c shows the FBP reconstruction of the F-22 aircraft fighter. Compared with the actual scaled model shown in fig. 3d, the outline shape of the F-22 model is clear and easily recognized.

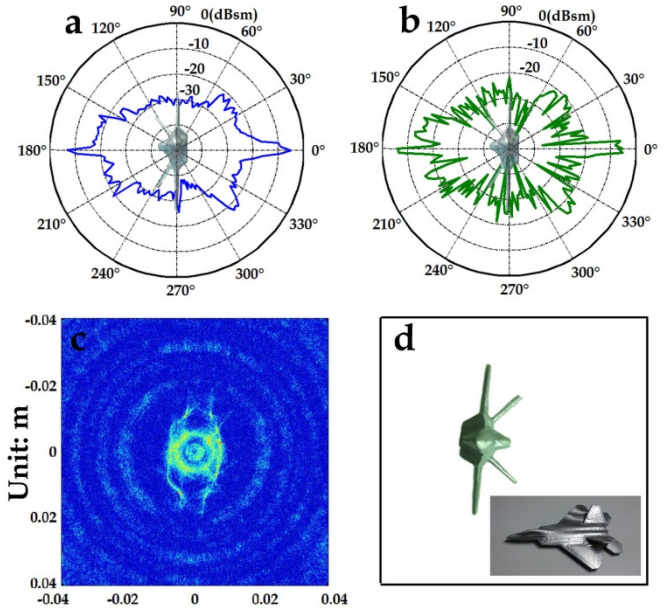

Fig. 3. (a) Frequency-averaged RCS of the model of aircraft F-22. (b) Frequency-resolved RCS of the scaled model at 0.6 THz. (d) cross section image reconstructed using the filtered back projection algorithm. (d) Metal 1:200 scaled model of F-22 aircraft fighter.

III. SUMMARY

We have experimentally constructed a time-domain THz radar system. Full 360° RCS measurement on scaled models of Liaoning aircraft carrier and F-22 aircraft fighter were performed. The application of an advanced filtered back projection algorithm allows the reconstruction of the two-dimensional imaging, which shows the distribution of the scattering points on the model. THz time domain radar will be a powerful candidate tool for THz scattering and imaging researches.

REFERENCES

[1].R. W. McGowan, R. A. Cheville and D. R. Grischkowsky, "Experimental study of the surface waves on a dielectric cylinder via terahertz impulse radar raging," *IEEE Trans. Microwave Theory & Tech.,* vol. 48, pp. 417, 2000.
[2].K. Iwaszczuk, H. Heiselberg and P. U. Jepsen, "Terahertz radar cross section measurements," *Opt. Express,* vol. 18, pp. 26399, 2010.
[3].J. Pearce, H. Choi, D. M. Mittleman, J. White, and D. Zimdars, "Terahertz wide aperture reflection tomography," *Opt. Lett.,* vol. 30, pp. 1653, 2005.
[4] .D. C. Liang, M. G. Wei, J. Q. Gu, et al., "Broad-band time domain terahertz radar cross-section research in scale models," Acta Physica Sinica, vol. 63, pp. 214102, 2014.